

New phosphorescent platinum(II) Schiff base complexes for PHOLED applications†

Jie Zhang,^a Fangchao Zhao,^b Xunjin Zhu,^{*a} Wai-Kwok Wong,^{*a} Dongge Ma^{*b} and Wai-Yeung Wong^{*a}

Received 11th April 2012, Accepted 6th June 2012

DOI: 10.1039/c2jm32266h

Some new symmetric and asymmetric platinum(II) Schiff base complexes with bulky substituents such as *tert*-butyl and triphenylamino groups have been synthesized which effectively reduced the aggregation or excimer formation. Using selected complexes as phosphorescent emitting materials, yellow light-emitting devices were fabricated with improved efficiency compared with the previously reported analogues. In addition, the phosphorescent white organic light-emitting device (WOLED) was fabricated using a single emissive layer composed of yellow- and blue-emitting materials.

Introduction

In 1987, a semiconducting organic small molecule was found by Tang and Van Slyke to be emissive with layered films under the application of an electric field.¹ In 1990, semiconducting conjugated polymers were also shown to emit green-yellow light under an electric field.² Since then, many efforts have been made to develop organic light-emitting devices (OLEDs). Although organic light-emitting devices have been commercialized as flat panel displays since 1997, only singlet excitons were utilized in this context. In order to harvest both singlet and triplet excitons for emission, heavy metal atoms have been incorporated into the emissive layer (EML) of OLEDs to increase the spin-orbit coupling and thereby facilitate the intersystem crossing from the singlet to the triplet excited states. After the premier work by Forrest, Thompson, and co-workers,³ some of the best materials arising from phosphorescent metal complexes, typically those composed of heavy metal ions, *e.g.* Ir(III),⁴ Pt(II),⁵ and Os(II),⁶ have been developed. In phosphorescent organic light-emitting devices (PHOLEDs) based on these materials, both singlet and

triplet excitons can be harnessed, theoretically approaching 100% internal quantum efficiency. Until now, cyclometalated iridium(III) complex is recognized as one of the best candidates of phosphorescent dyes with high quantum yields due to the short lifetime of triplet excited states.^{4f} Apart from the Ir(III) systems, platinum(II) complexes have also been extensively studied to construct PHOLEDs. Cyclometalated platinum(II) C[^]N[^]N complexes of 6-phenyl-2,2'-bipyridine and N[^]C[^]N complexes of 1,3-dipyridyl-benzene have been reported to display strong phosphorescence and electrophosphorescence.^{5e} Recently, Che *et al.* developed highly blue phosphorescent Pt(II) complexes based on tetradentate ligands with a bis(NHC) dianionic feature (NHC = N-heterocyclic carbene), which demonstrated that incorporation of NHC, a strong σ -donor but poor π -acceptor, into the cyclometalated Pt(II) complexes can shorten the ligand π -conjugation lengths and consequently broaden the energy gaps.⁷ Che and co-workers have also demonstrated that platinum(II) Schiff base complexes could be used for high-performance OLEDs.⁸ At low dopant concentrations (<5.0 wt%) of platinum(II) Schiff base complexes, the device efficiency was increased. However, at higher dopant concentrations (>5.0 wt%), aggregate/excimer formation was found to reduce the device efficiency and affect the color purity.

In this report, we designed and synthesized some new symmetric and asymmetric platinum(II) Schiff base complexes with bulky substituents such as *tert*-butyl and triphenylamino groups, which effectively reduced the aggregation or excimer formation and subsequently improved the performance of PHOLEDs. In addition, the phosphorescent white organic light-emitting device (WOLED) was fabricated using a single EML composed of yellow and blue emitting materials. Though the efficiency of PHOLEDs based on these platinum(II) Schiff base complexes cannot compete with Ir(III) systems, they are still attractive because of their preparative accessibility and thermal stability, and would provide access to new classes of phosphorescent materials of practical interest.

^aInstitute of Molecular Functional Materials (Areas of Excellence Scheme, University Grants Committee, Hong Kong) and Department of Chemistry and Institute of Advanced Materials, Hong Kong Baptist University, Waterloo Road, Hong Kong, P. R. China. E-mail: xjzhu@hkbu.edu.hk; wkwong@hkbu.edu.hk; rwywong@hkbu.edu.hk; Fax: +86 852 3411 7348; Tel: +86 852 3411 5157

^bState Key Laboratory of Polymer Physics and Chemistry, Changchun Institute of Applied Chemistry, Chinese Academy of Sciences, Changchun, P. R. China. E-mail: mdg1014@ciac.jl.cn; Fax: +86 431 8526 2873; Tel: +86 431 8526 2357

† Electronic supplementary information (ESI) available. Crystal data for **2b**. C₂₈H₃₄Br₂N₂O₂Pt, monoclinic, space group C2/c, *a* = 29.187(4), *b* = 13.372(2), *c* = 15.048(2) Å, β = 109.333(2)°, *V* = 5542(1) Å³, *Z* = 8, *D_c* = 1.883 g cm⁻³, μ (Mo-K α) = 7.975 mm⁻¹, *F*(000) = 3040, *T* = 173(2) K. *R*1 = 0.0461, *wR*2 = 0.1076 for 4743 independent reflections with a goodness-of-fit of 1.069. The data were collected on a Bruker Smart 1000 CCD diffractometer and the structure was solved using the program SHELXLTL. CCDC 875500. For ESI and crystallographic data in CIF or other electronic format see DOI: 10.1039/c2jm32266h

Results and discussion

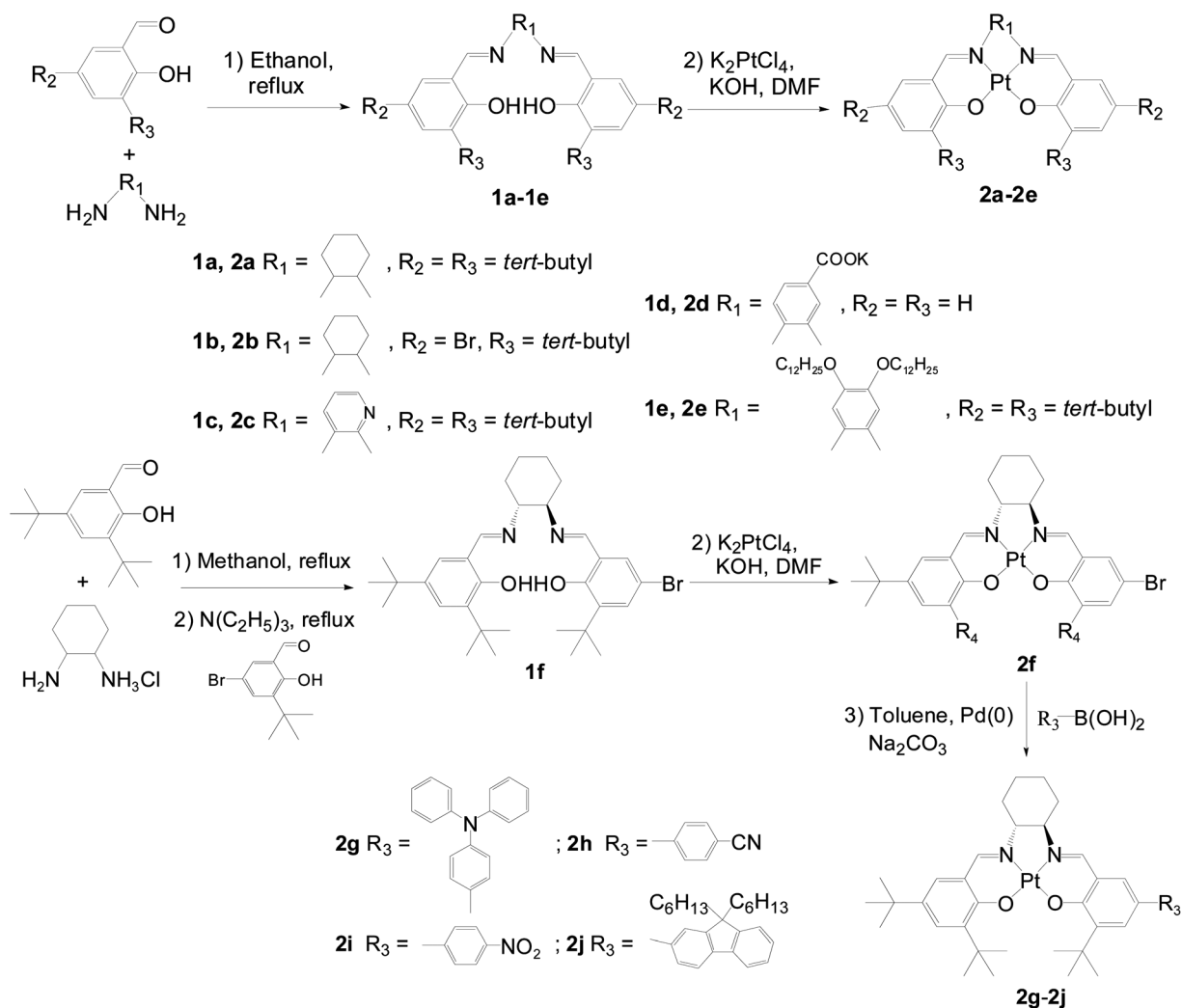
Synthetic procedures and chemical characterization

The Schiff base ligands (**1a–1e**) were easily prepared in good yields (62–85%) *via* condensation of the substituted 2-hydroxybenzaldehydes with diamines (Scheme 1).⁹ The Schiff base ligands were purified by recrystallization and then reacted with K_2PtCl_4 and KOH in DMF at 70 °C overnight. A yellow solid was precipitated from the solution when water was added. The crude solid was filtered and purified on a silica gel column using CH_2Cl_2 and hexane as the eluent to give orange (salen complexes) or red (salophen complexes) target complexes.^{8,10} On the other hand, the synthesis of asymmetric salen has proven to be challenging. Based on a straightforward one-pot protocol reported recently by Jones *et al.*, asymmetric salen ligands can be prepared efficiently on gram scales.¹¹ The first condensation between *trans*-1,2-diamino-cyclohexane mono-(hydrogen chloride) and 3,5-di-*tert*-butyl-2-hydroxy-benzaldehyde was carried out in a 1 : 1 (v/v) mixture of anhydrous methanol and ethanol at ambient temperature. Activated 4 Å molecular sieves were added to remove the water formed during the reaction. After the first condensation was completed within about 4 h, a solution of

5-bromo-3-*tert*-butyl-2-hydroxybenzaldehyde in dichloromethane was added to the former reaction systems, followed by the slow addition of an excess amount of anhydrous triethylamine as a deprotection base. The target asymmetric salen ligand **1f** was isolated in 60–85% yield as a light yellow solid by means of column chromatography on a silica gel pretreated with methanol or methanol–triethylamine. Also, treating **1f** with K_2PtCl_4 in DMF solution afforded the corresponding platinum(II) Schiff base complex **2f** in 36% yield. Based on **2f**, the other unsymmetrical platinum(II) Schiff base complexes **2g–2j** were obtained in moderate yields (58–74%) *via* Suzuki–Miyaura reactions between **2f** and different types of boronic acid with bulky substituents.

All the new symmetric and asymmetric Schiff base ligands and their corresponding platinum(II) complexes were characterized by 1H NMR, IR, MS, UV-Vis spectrum and elemental analysis.

The 1H NMR spectrum of the symmetric Schiff base ligands **1a**, **1b** and **1e** in $CDCl_3$ exhibits a broad singlet at δ 13.72, 13.86 and 13.66 ppm for the O–H protons, respectively. The chemical shift is typical for the resonance-assisted hydrogen bonded (RAHB) proton of O–H \cdots N=C. The other characteristic imino protons of the ligands **1a**, **1b** and **1e** appear as sharp singlet at δ



Scheme 1 Synthesis of symmetrical and unsymmetrical platinum(II) Schiff base complexes **2a–2j**.

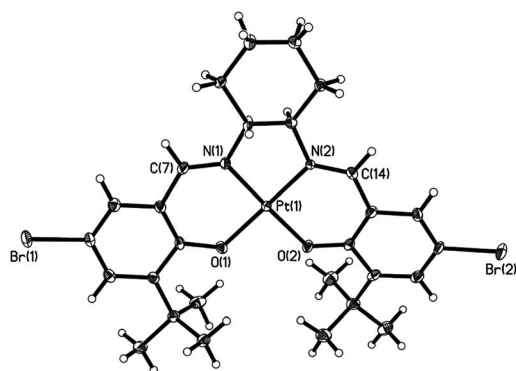


Fig. 1 A perspective view of **2b**. Selected bond lengths (Å): Pt(1)–N(1) 1.944(6), Pt(1)–N(2) 1.943(6), Pt(1)–O(1) 1.988(5), Pt(1)–O(2) 1.997(4). Selected bond angles (°): N(1)–Pt(1)–N(2) 83.7(2), N(1)–Pt(1)–O(1) 95.0(2), N(2)–Pt(1)–O(2) 94.9(2), O(1)–Pt(1)–O(2) 86.5(19), N(2)–Pt(1)–O(1) 177.4(2), N(1)–Pt(1)–O(2) 177.8(2).

8.30, 8.17 and 8.63 ppm, respectively. On the other hand, the ^1H NMR spectrum of the asymmetric Schiff base ligand **1c** shows two broad singlets at δ 13.81 and 13.45 ppm for the O–H protons and two sharp singlets at δ 9.52 and 8.70 ppm for the imino protons. The ^1H NMR spectrum of symmetric platinum(II) Schiff base complexes **2a**, **2b** and **2e** in CDCl_3 exhibits a singlet at δ 8.07, 7.96 and 8.61 ppm for the imino protons, respectively. The ^1H NMR spectrum of the asymmetric platinum(II) Schiff base complex **2c** in CDCl_3 exhibits a singlet for each of the two different imino protons in the range of δ 7.93–9.64 ppm.

The IR absorption peak between 1627 and 1641 cm^{-1} can be assigned to the C=N stretching vibration, and the absorption peak at 2224 cm^{-1} of **2h** to the C \equiv N stretching vibration. The MALDI-TOF-MS spectra of platinum(II) complexes exhibit the $[\text{M}]^+$ or $[\text{M} + \text{H}]^+$ peaks at m/z values which are deviated less than 9 ppm from the theoretical values.

Complex **2b** was also characterized by X-ray crystallography (Fig. 1). The Pt(II) ion coordinates to two N atoms and two O

atoms in a square planar geometry. The average Pt–N and Pt–O distances are 1.944 and 1.992 Å, respectively. Thanks to the bulky *tert*-butyl substituents, the closest Pt(II)⋯Pt(II) distance is 4.976 Å, which is outside the range of 2.7–3.5 Å for any metal-philic interaction. Moreover, the presence of the bulky groups effectively inhibits intermolecular π – π stacking interactions of the aryl rings.

Photophysical and thermal properties

The UV-Vis absorption spectra of **1a–1j** are very similar and are characteristic of intraligand transitions of Schiff base ligands (Fig. S1† in the ESI).⁹ The UV-Vis absorption spectral data of platinum(II) complexes **2a–2j** are listed in Table 1. In CH_2Cl_2 , the absorption spectra of **2a**, **2b**, and **2f–2j**, having the aliphatic R_1 motif, are similar to each other (Fig. 2a and b). Each of them exhibits intense high-energy absorption bands at $\lambda_{\text{max}} = 253$ –352 nm and moderately intense absorption bands at $\lambda_{\text{max}} = 425$ –441 nm, which can be assigned to intraligand π – π^* (200–400 nm) and metal-to-ligand charge-transfer (MLCT, $[\text{Pt}(5d) \rightarrow \pi^*(\text{L})]$) mixed with intraligand $[\text{one pair (phenoxide)} \rightarrow \pi^*(\text{imine})]$ transitions (400–600 nm), respectively.⁸ Complexes with the phenylene R_1 motif (**2c–2e**) show two high-energy absorptions with peak maxima at $\lambda_{\text{max}} = 368$ –393 nm, moderately intense absorption bands at $\lambda_{\text{max}} = 476$ –555 nm, which are red-shifted compared with the aliphatic R_1 bridged platinum(II) complexes (**2a**, **2b**, **2f–2j**) due to the expansion of π -conjugation (Fig. 2a). The absorptions of these complexes are similar, which indicate that the substituents on the Schiff base ligands only have a little effect on the energy of absorption.

The emission spectra of **2a–2j** at 298 K are depicted in Fig. 3 and the photophysical data are summarized in Table 1. Intense emission bands with λ_{max} at 557–568 nm ($\Phi_{\text{em}} = 0.11$ –0.20; $\tau = 2.60$ –12.80 μs) are observed upon excitation of the platinum(II) complexes with an aliphatic R_1 motif (**2a**, **2b**, **2f**, **2g**, **2h**, **2j**) at 400 nm in CH_2Cl_2 at 298 K, while **2i** shows very weak luminescence ($\Phi_{\text{em}} = 0.0071$) with λ_{max} at 556 nm due to the electron

Table 1 Summary of UV-visible absorption and luminescent data of complexes **2a–2j** at room temperature in CH_2Cl_2 (1.0×10^{-5} M)

Compound	Absorption, $\lambda_{\text{max}}/\text{nm}$ [$\log(\epsilon\text{ dm}^{-3}\text{ mol}^{-1}\text{ cm}^{-1})$] ^a	Luminescence, λ_{max} (nm) at 298 K	Luminescence, λ_{max} (nm) at 77 K ^b	Φ_{em} ^c	τ (μs), 298 K	τ (μs), 77 K
2a	253 (4.59), 316 (4.09), 353 (4.15), 437 (3.74)	560, 602 (sh)	551, 599	0.15	3.36	9.65
2b	261 (4.62), 322 (4.08), 351 (4.10), 441 (3.74)	559, 603 (sh)	563, 609	0.18	4.89	11.56
2c	258 (4.47), 373 (4.37), 389 (4.47), 486 (3.78), 561 (3.78)	650	663, 736 (sh)	0.12	2.60	13.73
2d	255 (4.33), 311 (3.90), 321 (3.94), 359 (4.18) 379 (4.22), 454 (3.14), 526 (3.30)	612, 673 (sh)	632	0.17	7.72	11.86
2e	262 (4.51), 330 (4.17), 373 (4.54), 392 (4.61) 497 (3.95), 556 (3.87)	590 (sh), 649	651, 724	0.11	2.85	8.98
2f	260 (4.69), 319 (4.16), 352 (4.17), 438 (3.77)	568, 612 (sh)	554, 602	0.15	3.94	10.33
2g	259 (4.27), 337 (4.43), 437 (3.48)	568	555, 603	0.17	6.34	11.18
2h	248 (4.33), 357 (4.37), 425 (3.59)	557, 596 (sh)	555, 604	0.16	8.39	9.25
2i	266 (3.61), 357 (4.30), 431 (4.32)	556	546, 559	0.007	12.80	19.69
2j	287 (4.28), 342 (4.50), 432 (3.67)	565, 608 (sh)	551, 592	0.20	5.37	10.23

^a Photophysical measurements were made with a concentration of 1×10^{-5} M in CH_2Cl_2 at room temperature. ^b Emission at 77 K was made in frozen CH_3CN at a concentration of 1×10^{-5} M. ^c Luminescence quantum yields (Φ_{em}) in degassed dichloromethane solution were determined with $[\text{Ru}(\text{bpy})_3](\text{PF}_6)_2$ (bpy = 2,2'-bipyridine) in acetonitrile as a standard reference solution ($\Phi_{\text{em}} = 0.062$).

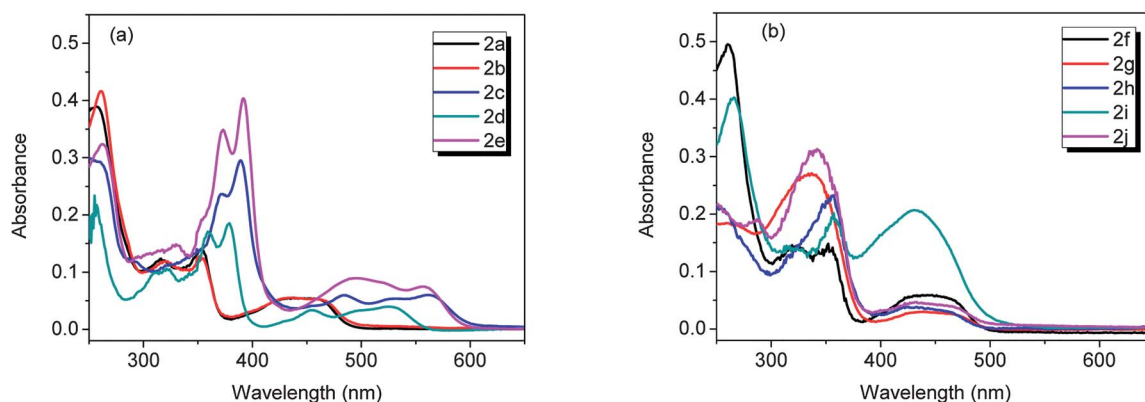


Fig. 2 UV-Vis absorption spectra of the Schiff base platinum(II) complexes **2a–2e** (a) and **2f–2j** (b) in CH_2Cl_2 (1.0×10^{-5} M).

deficient nitro group. Those platinum(II) complexes (**2c**, **2e**) bridged by the phenylene R_1 motif show red emission with bands at $\lambda_{\text{max}} = 650, 649$ nm and quantum yields and lifetimes of $\Phi_{\text{em}} = 0.12, 0.11$ and $\tau = 2.60, 2.85$ μs , respectively. The platinum(II) complex (**2d**) bridged by the pyridyl R_1 motif shows an orange emission at $\lambda_{\text{max}} = 612$ nm ($\Phi_{\text{em}} = 0.17$; $\tau = 7.72$ μs). The decay time in the microsecond scale indicates that the emission band originates from the triplet emissive excited state.^{8b} It is noteworthy that when **2g** and **2j** are excited at 300 and 380 nm, respectively, only emissions corresponding to the platinum(II) complexes are observed. The singlet excited emission of triphenylamine or fluorene segment is quenched, which indicates an efficient intramolecular energy transfer from triphenylamine or fluorene to the Schiff base platinum(II) complexes.¹² The platinum(II) complexes **2a**, **2b**, **2f**, **2g**, **2h** and **2j**, based on aliphatic R_1 motif bridged symmetric and asymmetric Schiff base ligands, show very similar emission wavelengths, while those based on electron-withdrawing group substituted Schiff base ligands (**2d**, **2h**, **2i**) show longer lifetimes. At 77 K, the emission spectra of the platinum(II) Schiff base complexes also show peaks in the visible range, which are consistent with the room temperature emission spectra despite the blue or red shift of the wavelengths. Furthermore, a longer lifetime was observed at 77 K (Fig. S2† in the ESI).

The thermal stabilities of **2a–2j** were investigated by the thermogravimetric analysis (TGA) method. All complexes are thermally stable with decomposition temperature in the range of 279–404 °C (Table 2).

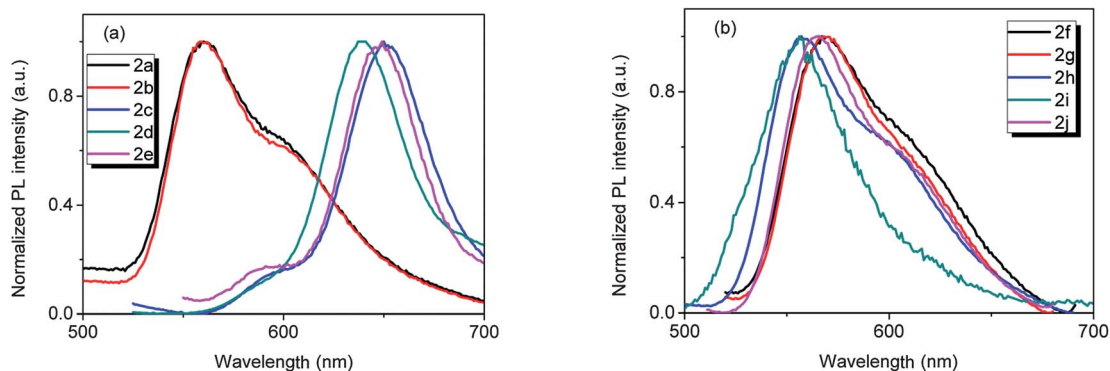


Fig. 3 Emission spectra of the platinum(II) Schiff base complexes **2a–2e** (a) and **2f–2j** (b) in CH_2Cl_2 (1.0×10^{-5} M) at room temperature.

Electrochemical studies

Cyclic voltammetry behaviour of platinum(II) Schiff base complexes was recorded in degassed CH_2Cl_2 at a scan rate of 100 mV s^{-1} with 0.1 M $[n\text{-Bu}_4\text{N}][\text{PF}_6]$ as the supporting electrolyte. All potentials are referenced to the ferrocenium–ferrocene (Fc–Fc^+) couple. A glassy carbon electrode was used as the working electrode, a platinum wire as the counter electrode and a Ag/AgCl as the reference electrode. Then the oxidation potentials of **2a–2j** were estimated *via* cyclic voltammetry to be in the range of 0.29–0.60 V. The HOMO was deduced by the equation $E_{\text{HOMO}} = -(E_{\text{ox}} + 4.80)$ eV. Estimated from the UV-visible absorption spectrum, the energy band gap of the platinum(II) complexes was obtained. Thus the LUMO was calculated to be the sum of the energy band gap and HOMO. The HOMO and LUMO levels of these complexes are in the range of -5.09 to -5.40 eV and -2.56 to -3.05 eV, respectively. The oxidation potentials and the HOMO–LUMO energy gap are summarized in Table 2.

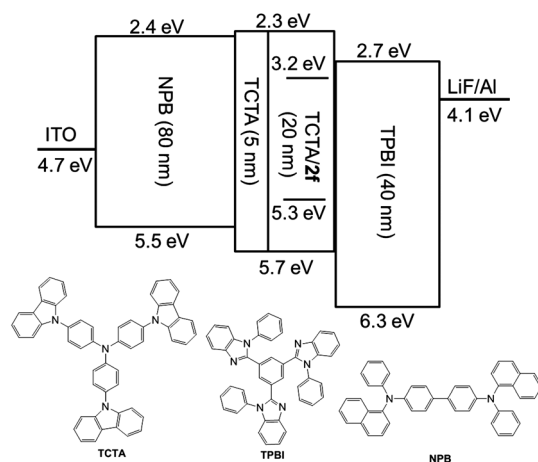
Electrophosphorescent OLED characterization

All of the new platinum(II) Schiff base complexes can be readily sublimed under vacuum which should be amenable to thermally evaporated OLED fabrication. Herein, to evaluate the performance of selected complexes as phosphorescent emitters, devices with the structure ITO/ MoO_3 (8 nm)/1,4-bis(1-naphthylphenylamino)-biphenyl (NPB) (80 nm)/4,4',4''-tri(9-carbazoyl)-triphenylamine (TCTA) (5 nm)/TCTA : x wt % Pt(II)

Table 2 Summary of cyclic voltammetry data and TGA of **2a–2j**

Compound	E_{ox}^a	HOMO ^b	LUMO ^c	E_g^d	T_d (°C)
2a	0.38	−5.18	−2.63	2.55	380
2b	0.29	−5.09	−2.56	2.53	330
2c	0.33	−5.13	−3.05	2.08	279
2d	0.30	−5.10	−2.89	2.21	388
2e	0.58	−5.38	−3.27	2.11	372
2f	0.60	−5.40	−2.88	2.52	336
2g	0.39	−5.19	−2.68	2.51	401
2h	0.32	−5.12	−2.58	2.54	341
2i	0.43	−5.23	−2.72	2.51	341
2j	0.33	−5.13	−2.61	2.52	404

^a Versus ferrocene–ferrocenium couples. ^b Estimated from the oxidation potentials HOMO = $-(E_{\text{ox}} + 4.80)$ eV. ^c Deduced from the HOMO and E_g . ^d Estimated from the UV-vis absorption spectra.

**Fig. 4** The device structure and energy level diagram of a OLED using **2f** as the emitting material.

complex (20 nm)/1,3,5-tri(1-phenyl-1*H*-benzo[*d*]imidazol-2-yl)phenyl (TPBI) (40 nm)/LiF (1 nm)/Al were fabricated as shown in Fig. 4. In the devices, the layers of NPB and TPBI were used as the hole- and electron-transporting layer, respectively. And TCTA was chosen as the host material because its emission spectrum overlaps with the absorption spectra of the platinum(II) complexes in this work. The selected platinum(II) Schiff base complexes with different dopant concentrations (4–12 wt%) in the host material TCTA served as the emissive layer. Another thin layer of TCTA was inserted between the emissive layer and the hole transporting layer, with LUMO of at least 0.3 eV above

that of the dopant and host, thus preventing electron leakage from the emissive layer. MoO₃ and LiF function as the hole- and electron-injecting layers, respectively. The indium tin oxide (ITO) coated glass substrate with 20 Ω per square sheet resistivity was used as the transparent anode.

The performances of the devices using **2a**, **2b**, **2c** and **2f** as electrophosphorescent dopant materials are summarized in Table 3. The EL spectra in the range of 500–800 nm well match the photoluminescence (PL) spectra of the corresponding complexes, revealing that EL emissions in this region come directly from the triplet excited state. The devices fabricated with complexes **2a**, **2b** and **2f** showed yellow emission with CIE coordinates at around (0.49, 0.51), while the devices with complex **2c** showed red emissions with CIE coordinates at around (0.68, 0.32). To optimize the device efficiency, concentration dependence experiments were carried out in the range of 6 to 12 wt%. At low platinum(II) dopant concentrations (≤ 8.0 wt%), the device efficiency was increased. It should be noted that aggregation/excimer formation was not obvious in our study even at high platinum(II) dopant concentrations of up to 12 wt%, and the slightly reduced device efficiency might arise from the triplet–triplet annihilation. As TCTA has a relatively higher triplet energy level,¹³ an efficient exothermic energy transfer from the TCTA triplet state to the triplet state of platinum(II) Schiff base complexes would occur given the perfect alignment of triplet state energy, leading to excellent triplet exciton confinement within the emissive layer. However, it is worth noting that incomplete electron trapping by the platinum(II) Schiff base complexes is evidenced by the observation of an EL band at 416 nm at low dopant concentrations, which primarily comes from the fluorescence of the host material TCTA.

The yellow OLED doped with 8 wt% **2a** shows an impressive performance with a turn-on voltage (V_{on}) of 3.5 V, a maximum brightness (L_{max}) of 10 826 cd m^{−2} at 13.5 V, a peak external quantum efficiency ($\eta_{\text{ext,max}}$) of 7.0%, a peak luminance efficiency ($\eta_{\text{L,max}}$) of 21 cd A^{−1} and a peak power efficiency ($\eta_{\text{p,max}}$) of 17 lm W^{−1} (Table 3). Another yellow light-emitting device with 8 wt% **2g** is also attractive in performance showing a better EL efficiency of 8.3%, 23 cd A^{−1} and 17 lm W^{−1}. This device turns on at 3.5 V and its light output can reach 11 106 cd m^{−2} at 13.7 V (Fig. 5a and b). Unlike most other platinum(II) systems,⁷ in which the EL was found to show significant spectral shifts upon dopant aggregation to give a broad red-shifted excimer emission, the EL spectra using **2a** or **2g** as dopant are found to be independent of the driving voltage from 4.5 to 15 V (Fig. 5c). The voltage-independent EL may be attributed to a lower tendency of complex **2a** or **2g** to form aggregates through Pt···Pt and/or π – π

Table 3 Summary of device performances at best dopant concentrations

Dopant	Dopant/wt%	V_{on}^a /V	L_{max}^b /cd m ^{−2}	$\eta_{\text{L,max}}^c$ /cd A ^{−1}	$\eta_{\text{p,max}}^d$ /lm W ^{−1}	$\eta_{\text{ext,max}}^e$ /%	EL _{max} ^f /nm	CIE, x, y
2a	8	3.5	10 826	21	17	7.0	560	0.49, 0.51
2b	10	3.7	1236	6.0	5.0	2.2	560	0.48, 0.51
2c	8	3.9	2468	1.3	0.9	2.4	656	0.68, 0.32
2g	8	3.5	11 106	23	17	8.3	564	0.50, 0.50
FIrpic and 2g	10 and 1	3.1	20 905	21	17	7.7	474, 500, 560	0.34, 0.44

^a Turn-on voltage. ^b Maximum luminance. ^c Maximum current efficiency. ^d Maximum power efficiency. ^e Maximum external quantum efficiency. ^f Peak emission wavelength.

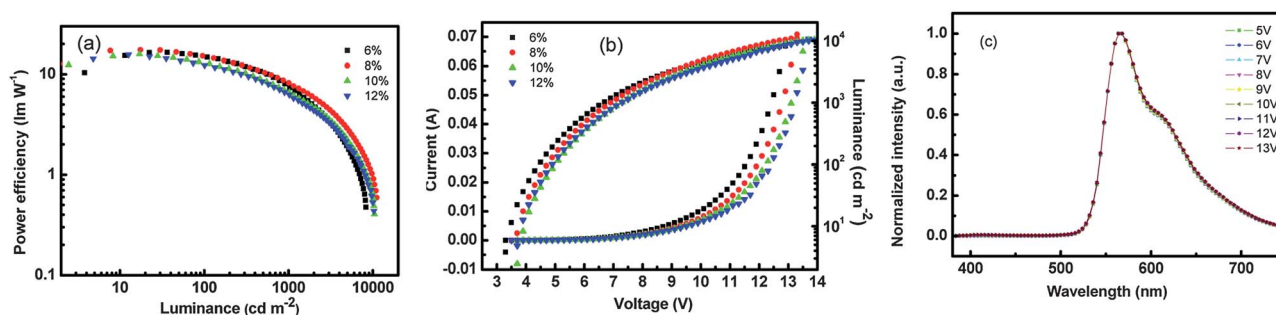


Fig. 5 (a) Performance of the OLED with **2g** as dopant: power efficiency–luminance curves; (b) current–voltage and luminance–voltage characteristics of the devices; (c) representative EL spectra of the OLED with 8 wt% dopant **2g** at the driving voltage from 5 to 13 V.

stacking interactions in the thin films. To the best of our knowledge, using **2a** or **2g** as the single EML, the device performance is remarkable and comparable to the ever reported analogous platinum(II) complexes as a single EML.¹⁴

White organic light-emitting devices (WOLEDs), especially fabricated with triplet emitters, show great promise for applications in flat-panel displays and solid-state lighting, because of their low operating voltage and the high brightness obtained.¹⁵ Inspired by the good device performance of the new platinum(II) Schiff base complex **2g**, we anticipate its great potential to obtain a white light emission by combining blue and yellow dopants in a single EML. Herein, a preliminary evaluation is given for WOLED that uses complex **2g** and bis(4,6-difluorophenylpyridine)(picolate) iridium(III) (FIrpic) in the device structure of ITO/MoO₃ (8 nm)/NPB (80 nm)/TCTA (5 nm)/TCTA : x% FIrpic : y% **2g** (20 nm)/TPBI (40 nm)/LiF (1 nm)/Al. The base device configuration is similar to the one shown in Fig. 4 with TCTA, NPB and TPBI as the host, hole- and electron-transporting materials, respectively. The device differs only in the composition of the EML, using a single EML with **2g** and FIrpic co-deposited from two separate sublimation sources. We determined through systematic variation that a device using 11 wt% dopants having a FIrpic/**2g** (blue/yellow) ratio of 10 : 1 gave the white emission as depicted in Fig. 6. The turn-on voltage for this device is 3.1 V and the light output can reach up to 20 905 cd m⁻² at 13.1 V. The $\eta_{\text{ext,max}}$ of 7.7%, $\eta_{\text{L,max}}$ efficiency of 21 cd A⁻¹ and $\eta_{\text{P,max}}$ of 17 lm W⁻¹ were obtained. The EL peak is voltage dependent, and increasing the applied voltage strengthens the proportion of blue emission with the corresponding CIE (0.40, 0.46) at 4 V and CIE (0.34, 0.44) at 9 V. Our primary results indicate that these platinum(II) Schiff bases are competitive candidates as phosphorescent dopant as yellow- or white-emitting OLED.

stacking interactions in the thin films. To the best of our knowledge, using **2a** or **2g** as the single EML, the device performance is remarkable and comparable to the ever reported analogous platinum(II) complexes as a single EML.¹⁴

Conclusions

We have developed a series of symmetrical and asymmetric phosphorescent platinum(II) Schiff base complexes with good thermal stability. These complexes with bulky substituents showed moderate emission quantum yields without obvious aggregation/excimer formation in solution or solid state. Using complexes **2a**, **2b** and **2g** as phosphorescent emitting materials, yellow light-emitting devices were fabricated with improved efficiency compared with other previously reported analogues. The maximum current efficiency, power efficiency, and brightness for the 8.0 wt% **2g** doped OLEDs are 23 cd A⁻¹, 17 lm W⁻¹ and 11 106 cd m⁻², respectively. Aggregation was successfully inhibited and the emission did not change even at high concentrations in the OLEDs. Given the synthetic simplicity and ease of structural variation, the preliminary results here indicate that these platinum(II) Schiff base complexes are good candidates for phosphorescent OLEDs. In addition, a single EML white-emitting device with a maximum efficiency of 7.7% and CIE coordinates of (0.34, 0.44) is also reported. The performance of yellow and white OLEDs using these complexes can be further enhanced by employing new matrix and carrier-transporting materials, and further investigation of the lifetime of the devices based on these platinum(II) Schiff bases is currently underway.

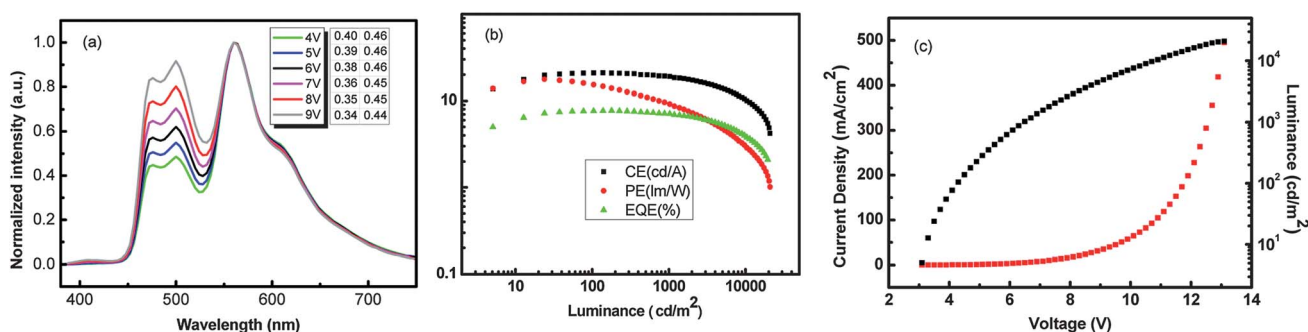


Fig. 6 Performance of WOLED using a single EML doped with **2g** and FIrpic: (a) EL spectrum; (b) power efficiency–luminance, luminescence efficiency–luminance and external quantum efficiency–luminance; (c) current–voltage and luminance–voltage characteristics of devices.

Experimental section

General information

The chemicals were purchased from Sigma-Aldrich Company and used as received. NMR spectra were recorded on a Bruker Ultrashield 400 Plus NMR spectrometer. The intermediates 5-bromo-3-*tert*-butyl-2-hydroxy-benzaldehyde¹⁶ and 4,5-bis(dodecyloxy)benzene-1,2-diamine¹⁷ were prepared according to the literature methods. High-resolution matrix-assisted laser desorption/ionization time-of-flight (MALDI-TOF) mass spectra were recorded with a Bruker Autoflex MALDI-TOF mass spectrometer and low-resolution FAB mass spectra with a Finnigan TSQ710 mass spectrometer. The C, H and N microanalyses were performed with a Carlo Erba 1106 elemental analyzer. The IR spectra (KBr pellets) were recorded with a Nicolet Magna 550 FTIR spectrometer. Electronic absorption spectra in the UV-Vis region were recorded on a Varian Cary 100 UV-Vis spectrophotometer, steady-state visible fluorescence and PL excitation spectra on a Photon Technology International (PTI) Alphascan spectrofluorimeter and visible decay spectra on a pico-N₂ laser system (PTI TimeMaster) with $\lambda_{\text{exc}} = 337$ nm. Luminescence quantum yields (Φ_{em}) in degassed dichloromethane solution were determined with [Ru(bpy)₃](PF₆)₂ (bpy = 2,2'-bipyridine) in acetonitrile as a standard reference solution ($\Phi_{\text{em}} = 0.062$) and calculated by $\Phi_{\text{s}} = \Phi_{\text{r}}(B_{\text{r}}/B_{\text{s}})(n_{\text{s}}/n_{\text{r}})^2(D_{\text{s}}/D_{\text{r}})$, where the subscripts r and s denote the reference standard and sample solution, respectively, and n , D , and Φ are the refractive index of the solvents, the integrated intensity, and the luminescence quantum yield, respectively. The quantity B is calculated by $B = 1 - 10^{-AL}$, where A is the absorbance at the excitation wavelength and L is the optical path length. Electrochemical measurements were made using a Princeton Applied Research model 273A potentiostat at a scan rate of 100 mV s⁻¹. A conventional three-electrode configuration consisting of a glassy carbon working electrode, a platinum wire counter electrode, and a Ag/AgCl reference electrode was used. The supporting electrolyte was 0.1 M [*n*-Bu₄N]PF₆ in THF. Ferrocene was added as a calibrant after each set of measurements, and all potentials reported were quoted with reference to the ferrocene-ferrocenium (Fc-Fc⁺) couple (taken as $E_{1/2} = +0.27$ V relative to the reference electrode). The HOMO was deduced by the equation $E_{\text{HOMO}} = -(E_{\text{ox}} + 4.80)$ eV, assuming that the energy level of ferrocene-ferrocenium to be -4.80 eV. Estimated from the UV-visible absorption spectrum, the energy band gap of the platinum(II) complexes was obtained. Thus the LUMO was calculated to be the sum of the energy band gap and HOMO.¹⁸ Thermal analyses were performed with Perkin-Elmer Pyris Diamond DSC and Perkin-Elmer TGA6 thermal analyzers.

OLED fabrication and measurement

The hole-injection MoO₃, hole-transporting material NPB (1,4-bis(1-naphthylphenylamino)-biphenyl) and TCTA (4,4',4''-tri(9-carbazolyl)-triphenylamine), and electron-transporting material TPBI (1,3,5-tri(1-phenyl-1*H*-benzo[*d*]imidazol-2-yl)phenyl) were commercially available. Commercial indium tin oxide (ITO) coated glass with a sheet resistance of 10 Ω sq⁻¹ was used as the starting substrate. Before device fabrication, the ITO glass substrates were pre-cleaned carefully and treated by UV/O₃ for 2

min. Then, the sample was transferred to the deposition system. 8 nm of MoO₃ was firstly deposited to the ITO substrate, followed by 80 nm NPB, 5 nm TCTA, 20 nm emissive and 40 nm TPBI layers. Finally, a cathode composed of 1 nm of lithium fluoride and 100 nm of aluminum was sequentially deposited onto the substrate under vacuum at 10⁻⁶ Torr to construct the device. The EL data were measured with a Keithley 2400 Source meter and a Keithley 2000 Source multimeter equipped with a calibrated silicon photodiode. The EL spectra were measured by a JY SPEX CCD3000 spectrometer. All measurements were carried out at room temperature under ambient conditions.

General procedure for the preparation of Schiff base ligands 1a–1e

To a stirred solution of one equivalent aliphatic or aromatic diamine in absolute ethanol, two equivalents of salicylaldehyde were added. The resulting mixture was refluxed overnight. After cooling to room temperature, the yellow product was precipitated out, and the product was filtered and washed with cold ethanol and petroleum ether (b.p. 30–40 °C).

1a: cyclohexane-1,2-diamine (443 mg, 3.89 mmol) and 3,5-di-*tert*-butyl-2-hydroxybenzaldehyde (2000 mg, 8.55 mmol) were used. Yield: 1807 mg (85%). ¹H NMR (400 MHz, CDCl₃): $\delta = 13.72$ (s, 2H, OH), 8.30 (s, 2H, C=NH), 7.30 (d, $J = 2.4$ Hz, 2H, Ar-H), 6.98 (d, $J = 2.4$ Hz, 2H, Ar-H), 3.38–3.26 (m, 2H, cyclohexane-H), 1.98–1.66 (m, 8H, cyclohexane-H), 1.41 (s, 18H, *tert*-butyl), 1.24 (d, $J = 6.7$ Hz, 18H, *tert*-butyl) ppm. IR (KBr): $\nu = 3435, 2952, 2865, 1630, 1595, 1469, 1439, 1361, 1270, 1174, 772$ and 644 cm⁻¹. FAB MS (positive mode): $m/z = 547$ [M + H]⁺.

1b: cyclohexane-1,2-diamine (40 mg, 0.35 mmol) and *tert*-butyl-bromobenzaldehyde (200 mg, 0.78 mmol) were used. Yield: 160 mg (77%). ¹H NMR (400 MHz, CDCl₃): $\delta = 13.86$ (s, 2H, OH), 8.17 (s, 2H, C=NH), 7.31 (d, $J = 2.4$ Hz, 2H, Ar-H), 7.08 (d, $J = 2.4$ Hz, 2H, Ar-H), 3.38–3.27 (m, 2H, cyclohexane-H), 1.89–2.01 (m, 4H, cyclohexane-H), 1.71–1.79 (m, 2H, cyclohexane-H), 1.45–1.50 (m, 2H, cyclohexane-H), 1.38 (s, 18H, *tert*-butyl) ppm. IR (KBr): $\nu = 3412, 2957, 2932, 2859, 1634, 1599, 1448, 1427, 1391, 1269, 1174, 772, 558$ cm⁻¹. HRMS (MALDI-TOF, positive mode, CH₂Cl₂): $m/z = 593.1196$ [M + H]⁺ (C₂₈H₃₆Br₂N₂O₂ + H: calcd 593.1198, $\Delta_m = -0.34$ ppm).

1c: pyridine-3,4-diamine (212 mg, 1.94 mmol) and 3,5-di-*tert*-butyl-2-hydroxybenzaldehyde (1000 mg, 4.27 mmol) were used. Yield: 758 mg (72%). ¹H NMR (400 MHz, CDCl₃): $\delta = 13.81$ (s, 1H, OH), 13.45 (s, 1H, OH), 9.52 (s, 1H, C=NH), 8.70 (s, 1H, C=NH), 8.39 (dd, $J = 4.7, 1.6$ Hz, 1H, Ar-H), 7.58 (dd, $J = 7.8, 1.6$ Hz, 1H, Ar-H), 7.49 (d, $J = 2.4$ Hz, 1H, Ar-H), 7.46 (d, $J = 2.4$ Hz, 1H, Ar-H), 7.36 (d, $J = 2.4$ Hz, 1H, Ar-H), 7.30–7.26 (m, 1H, Ar-H), 7.23 (d, $J = 2.4$ Hz, 1H), 1.50 (s, 9H, *tert*-butyl), 1.42 (s, 9H, *tert*-butyl), 1.33 (s, 9H, *tert*-butyl), 1.32 (s, 9H, *tert*-butyl) ppm. IR (KBr): $\nu = 3435, 2955, 2907, 1614, 1589, 1556, 1454, 1433, 1359, 1272, 1172, 773, 675$ cm⁻¹. HRMS (MALDI-TOF, positive mode, CH₂Cl₂): $m/z = 542.3751$ [M + H]⁺ (C₃₅H₄₇N₃O₂ + H: calcd 542.3741, $\Delta_m = 1.84$ ppm).

1d: 3,4-diaminobenzoic acid (566 mg, 3.73 mmol) and 2-hydroxybenzaldehyde (1000 mg, 8.20 mmol) were used. Yield: 1049 mg (78%). ¹H NMR (400 MHz, [D₆]DMSO): $\delta = 13.13$ (s, 1H, COOH), 12.80 (s, 1H, OH), 12.57 (s, 1H, OH), 9.03 (s, 1H, C=NH), 8.97 (s, 1H, C=NH), 7.98 (d, $J = 1.8$ Hz, 1H, Ar-H),

7.94 (dd, $J = 8.2, 1.8$ Hz, 1H, Ar-*H*), 7.71 (td, $J = 7.8, 1.4$ Hz, 2H, Ar-*H*), 7.52 (d, $J = 8.2$ Hz, 1H, Ar-*H*), 7.43 (qd, $J = 8.2, 1.6$ Hz, 2H, Ar-*H*), 7.01–6.91 (m, 4H, Ar-*H*) ppm. IR (KBr): $\nu = 3435, 2959, 2857, 1683, 1615, 1592, 1559, 1453, 1432, 1361, 1278, 1193, 761, 679$ cm⁻¹. HRMS (MALDI-TOF, positive mode, CH₂Cl₂): $m/z = 361.1176$ [M]⁺ (C₂₁H₁₆N₂O₄: calcd 361.1183, $\Delta_m = -1.94$ ppm).

1e: 4,5-bis(dodecyloxy)benzene-1,2-diamine (463 mg, 0.97 mmol) and 3,5-di-*tert*-butyl-2-hydroxybenzaldehyde (500 mg, 2.14 mmol) were used. Yield: 547 mg (62%). ¹H NMR (400 MHz, CDCl₃): $\delta = 13.66$ (s, 2H, OH), 8.63 (s, 2H, C=NH), 7.41 (d, 2H, $J = 2.4$ Hz, Ar-*H*), 7.20 (d, 2H, $J = 2.4$ Hz, Ar-*H*), 6.81 (s, 2H, Ar-*H*), 4.07 (m, 4H, -OCH₂-), 1.84–1.88 (m, 4H, -OCH₂CH₂-), 1.49–1.56 (m, 6H), 1.43 (s, 18H, *tert*-butyl), 1.35 (m, 4H), 1.32 (s, 18H, *tert*-butyl), 1.27 (m, 26H), 0.88 (s, 6H, -CH₃) ppm. IR (KBr): $\nu = 3435, 2955, 2924, 1615, 1579, 1513, 1472, 1439, 1361, 1263, 1173, 773, 686$ cm⁻¹. HRMS (MALDI-TOF, positive mode, CH₂Cl₂): $m/z = 909.7403$ [M + H]⁺ (C₂₁H₁₆N₂O₄: calcd 361.1183, $\Delta_m = -4.51$ ppm).

Preparation of asymmetric Schiff base ligand 1f

A solution of 3,5-di-*tert*-butyl-2-hydroxybenzaldehyde (1000 mg, 4.27 mmol), *trans*-diaminocyclohexane mono(hydrogen chloride) (645 mg, 4.27 mmol) and 4 Å molecular sieves (500 mg) in anhydrous methanol (15 mL) were stirred overnight at room temperature under nitrogen. Then, 5-bromo-3-*tert*-butyl-2-hydroxybenzaldehyde (1098 mg, 4.27 mmol) in anhydrous CH₂Cl₂ (20 mL) and anhydrous NEt₃ (863 mg, 8.54 mmol) were added. The mixture was stirred at room temperature for an additional 10 h. The residue after solvent evaporation was purified by silica-gel column chromatography using a solvent mixture of hexane and CH₂Cl₂ as the eluent to give a yellow solid of **1f**. Yield: 1632 mg (67%). ¹H NMR (400 MHz, CDCl₃): $\delta = 13.95$ (s, 1H, OH), 13.59 (s, 1H, OH), 8.26 (s, 1H, C=NH), 8.18 (s, 1H, C=NH), 7.31 (s, 1H, Ar-*H*), 7.28 (s, 1H, Ar-*H*), 7.08 (s, 1H, Ar-*H*), 6.94 (s, 1H, Ar-*H*), 3.30 (m, 2H, cyclohexane-*H*), 1.73–1.95 (m, 8H, cyclohexane-*H*), 1.42 (s, 9H, *tert*-butyl), 1.37 (s, 9H, *tert*-butyl), 1.23 (s, 9H, *tert*-butyl) ppm. IR (KBr): $\nu = 3429, 2956, 2862, 1629, 1469, 1439, 1361, 1272, 1174, 772, 644$ cm⁻¹. FAB MS (positive mode): $m/z = 570$ [M]⁺.

General procedure for the preparation of platinum(II) Schiff base complexes 2a–2f

A solution of one equivalent of the Schiff base ligand **1** and two equivalents of KOH was stirred about 0.5 h in DMF under nitrogen at 70 °C. Then, excess K₂PtCl₄ in DMSO (5 mL) was added and continuously stirred for 24 h under nitrogen at 70 °C. The reaction mixture was extracted with CH₂Cl₂ and washed with water several times. The residue after solvent evaporation was purified by silica-gel column chromatography using a solvent mixture of hexane and CH₂Cl₂ as eluent to give an orange solid.

2a: Schiff base ligand **1a** (100 mg, 0.18 mmol), KOH (21 mg, 0.37 mmol) and K₂PtCl₄ (91 mg, 0.22 mmol) were used. Yield: 51 mg (38%). ¹H NMR (400 MHz, CDCl₃): $\delta = 8.07$ (s, 2H, C=NH), 7.56 (d, 2H, $J = 2.4$ Hz, Ar-*H*), 7.08 (d, 2H, $J = 2.4$ Hz, Ar-*H*), 3.43–3.45 (m, 2H, cyclohexane-*H*), 2.65–2.68 (m, 2H,

cyclohexane-*H*), 1.92–1.94 (m, 2H, cyclohexane-*H*), 1.52–1.53 (m, 20H, cyclohexane-*H* and *tert*-butyl), 1.40–1.41 (m, 2H, cyclohexane-*H*), 1.29 (s, 18H, *tert*-butyl) ppm. IR (KBr): $\nu = 3435, 2952, 2866, 1610, 1528, 1433, 1319, 1254, 1168, 781$ and 545 cm⁻¹. HRMS (MALDI-TOF, positive mode, CH₂Cl₂): $m/z = 739.3687$ [M]⁺ (C₃₆H₅₂N₂O₂Pt: calcd 739.3674, $\Delta_m = -1.76$ ppm). UV-Vis (CH₂Cl₂, 20 °C): λ_{\max} [log(ϵ dm⁻³ mol⁻¹ cm⁻¹)] = 253 (4.59), 316 (4.09), 353 (4.15), 437 (3.74) nm. C₃₆H₅₂N₂O₂Pt·0.5H₂O (748.9): calcd C 57.74, H 7.13, N 3.74; found: C 57.44, H 7.08, N 3.79%.

2b: Schiff base ligand **1b** (100 mg, 0.17 mmol), KOH (19 mg, 0.34 mmol) and K₂PtCl₄ (84 mg, 0.20 mmol) were used. Yield: 34 mg (26%). ¹H NMR (400 MHz, CDCl₃): $\delta = 7.96$ (s, 2H, C=NH), 7.50 (d, 2H, $J = 2.8$ Hz, Ar-*H*), 7.28 (d, 2H, $J = 2.6$ Hz, Ar-*H*), 3.50–3.53 (m, 2H, cyclohexane-*H*), 2.59–2.62 (m, 2H, cyclohexane-*H*), 1.88–1.91 (m, 2H, cyclohexane-*H*), 1.51–1.52 (m, 2H, cyclohexane-*H*), 1.48 (m, 18H, *tert*-butyl), 1.30–1.36 (m, 2H, cyclohexane-*H*) ppm. IR (KBr): $\nu = 3436, 2944, 2867, 1623, 1526, 1429, 1313, 1257, 1164, 778$ and 582 cm⁻¹. HRMS (MALDI-TOF, positive mode, CH₂Cl₂): $m/z = 786.0629$ [M]⁺ (C₂₈H₃₄Br₂N₂O₂Pt: calcd 786.0609, $\Delta_m = 2.54$ ppm). UV-Vis (CH₂Cl₂, 20 °C): λ_{\max} [log(ϵ dm⁻³ mol⁻¹ cm⁻¹)] = 261 (4.62), 322 (4.08), 351 (4.10), 441 (3.74) nm. C₂₈H₃₄Br₂N₂O₂Pt (785.47): calcd C 42.82, H 4.36, N 3.57; found: C 42.69, H 4.55, N 3.52%.

2c: Schiff base ligand **1c** (100 mg, 0.18 mmol), KOH (21 mg, 0.37 mmol) and K₂PtCl₄ (92 mg, 0.22 mmol) were used. Yield: 96 mg (71%). ¹H NMR (400 MHz, CDCl₃): $\delta = 9.64$ (s, 1H, C=NH), 8.87 (s, 1H, C=NH), 8.37 (dd, 1H, $J = 4.4, 0.8$ Hz, Ar-*H*), 8.29 (dd, 1H, $J = 8.8, 0.8$ Hz, Ar-*H*), 7.70 (td, 2H, $J = 1.6, 0.8$ Hz, Ar-*H*), 7.47 (d, 1H, $J = 2.0$ Hz, Ar-*H*), 7.31 (d, 1H, $J = 2.0$ Hz, Ar-*H*), 7.17 (dd, 1H, $J = 8.0, 4.8$ Hz, Ar-*H*), 1.59 (s, 18H, *tert*-butyl), 1.35 (s, 18H, *tert*-butyl) ppm. IR (KBr): $\nu = 3435, 2953, 2867, 1598, 1519, 1441, 1360, 1268, 1170, 782$ and 542 cm⁻¹. HRMS (MALDI-TOF, positive mode, CH₂Cl₂): $m/z = 735.3263$ [M + H]⁺ (C₃₅H₄₅N₃O₂Pt: calcd 735.3235, $\Delta_m = 3.81$ ppm). UV-Vis (CH₂Cl₂, 20 °C): λ_{\max} [log(ϵ dm⁻³ mol⁻¹ cm⁻¹)] = 258 (4.47), 373 (4.37), 389 (4.47), 486 (3.78), 561 (3.78) nm. C₃₅H₄₅N₃O₂Pt·1/3CH₂Cl₂ (763.14): calcd C 55.61, H 6.03, N 5.51; found: C 55.44, H 5.89, N 5.57%.

2d: Schiff base ligand **1d** (100 mg, 0.28 mmol), KOH (31 mg, 0.55 mmol) and K₂PtCl₄ (138 mg, 0.33 mmol) were used. Yield: 112 mg (68%). ¹H NMR (400 MHz, [D₆]DMSO): $\delta = 9.60$ (s, 1H, C=NH), 9.57 (s, 1H, C=NH), 8.40 (s, 1H, Ar-*H*), 8.37 (d, 1H, $J = 8.8$ Hz, Ar-*H*), 8.10 (dd, 1H, $J = 8.4, 0.8$ Hz, Ar-*H*), 7.94 (td, 2H, $J = 7.8, 2.0$ Hz, Ar-*H*), 7.58–7.64 (m, 2H, Ar-*H*), 7.16 (d, 2H, $J = 4.0$ Hz, Ar-*H*), 6.83 (qd, 2H, $J = 8.0, 0.6$ Hz, Ar-*H*) ppm. IR (KBr): $\nu = 3429, 2953, 1612, 1524, 1385, 1366, 1253, 1183, 779$ and 545 cm⁻¹. HRMS (MALDI-TOF, positive mode, CH₂Cl₂): $m/z = 591.9498$ [M]⁺ (C₂₁H₁₃KN₂O₄Pt: calcd 591.5152, $\Delta_m = 7.34$ ppm). UV-Vis (DMSO, 20 °C): λ_{\max} [log(ϵ dm⁻³ mol⁻¹ cm⁻¹)] = 255 (4.33), 311 (3.90), 321 (3.94), 359 (4.18), 379 (4.22), 454 (3.14), 526 (3.30) nm. C₂₁H₁₃KN₂O₄Pt (591.52): calcd C 42.64, H 2.22, N 4.74; found: C 42.53, H 2.32, N 4.89%.

2e: Schiff base ligand **1e** (200 mg, 0.22 mmol), KOH (25 mg, 0.44 mmol) and K₂PtCl₄ (110 mg, 0.26 mmol) were used. Yield: 75 mg (31%). ¹H NMR (400 MHz, CDCl₃): $\delta = 8.61$ (s, 2H, C=NH), 7.63 (s, 2H, Ar-*H*), 7.36 (s, 2H, Ar-*H*), 7.31 (s, 2H, Ar-*H*), 4.14 (m, 4H, -OCH₂-), 1.91 (m, 4H, -OCH₂CH₂-), 1.57 (s, 18H, *tert*-butyl), 1.27–1.41 (m, 54H), 0.88 (s, 6H, -CH₃) ppm. IR

(KBr): $\nu = 3435, 2952, 2852, 1606, 1585, 1515, 1463, 1358, 1275, 1167, 781$ and 545 cm^{-1} . HRMS (MALDI-TOF, positive mode, CH_2Cl_2): $m/z = 1102.7044 [\text{M}]^+$ ($\text{C}_{60}\text{H}_{94}\text{N}_2\text{O}_4\text{Pt}$: calcd $1102.6938, \Delta_m = 9.52$ ppm). UV-Vis ($\text{CH}_2\text{Cl}_2, 20^\circ\text{C}$): $\lambda_{\text{max}} [\log(\epsilon \text{ dm}^{-3} \text{ mol}^{-1} \text{ cm}^{-1})] = 262 (4.51), 330 (4.17), 373 (4.54), 392 (4.61), 497 (3.95), 556 (3.87)$ nm. $\text{C}_{60}\text{H}_{94}\text{N}_2\text{O}_4\text{Pt}$ (1102.48): calcd C 65.37, H 8.59, N 2.54; found: C 65.40, H 8.63, N 2.71%.

2f: Schiff base ligand **1f** (2000 mg, 3.51 mmol), KOH (393 mg, 7.02 mmol) and K_2PtCl_4 (1747 mg, 4.21 mmol) were used. Yield: 964 mg (36%). $^1\text{H NMR}$ (400 MHz, CDCl_3): $\delta = 8.01$ (s, 1H, C=NH), 7.93 (s, 1H, C=NH), 7.58 (d, $J = 2.5$ Hz, 1H, Ar-H), 7.48 (d, $J = 2.5$ Hz, 1H, Ar-H), 7.21 (d, $J = 2.5$ Hz, 1H, Ar-H), 7.09 (d, $J = 2.5$ Hz, 1H, Ar-H), 3.49–3.60 (m, 2H, cyclohexane-H), 2.53–2.62 (m, 2H, cyclohexane-H), 1.82–1.85 (m, 2H, cyclohexane-H), 1.51 (s, 9H, *tert*-butyl), 1.48–1.49 (m, 11H, cyclohexane-H and *tert*-butyl), 1.28–1.31 (m, 11H, cyclohexane-H and *tert*-butyl) ppm. IR (KBr): $\nu = 3436, 2950, 2866, 1613, 1528, 1431, 1315, 1254, 1166, 779$ and 582 cm^{-1} . HRMS (MALDI-TOF, positive mode, CH_2Cl_2): $m/z = 763.2203 [\text{M} + \text{H}]^+$ ($\text{C}_{32}\text{H}_{43}\text{BrN}_2\text{O}_2\text{Pt} + \text{H}$: calcd $763.2217, \Delta_m = -1.83$ ppm). UV-Vis ($\text{CH}_2\text{Cl}_2, 20^\circ\text{C}$): $\lambda_{\text{max}} [\log(\epsilon \text{ dm}^{-3} \text{ mol}^{-1} \text{ cm}^{-1})] = 260 (4.69), 319 (4.16), 352 (4.17), 438 (3.77)$ nm. $\text{C}_{32}\text{H}_{43}\text{BrN}_2\text{O}_2\text{Pt}$ (762.68): calcd C 50.39, H 5.68, N 3.67; found: C 50.42, H 5.73, N 3.49%.

General procedure for the preparation of platinum(II) asymmetric Schiff base complexes **2g–2j**

A suspension of **2f**, 1.2 equivalent of boronic acid functionalized reagent, 3 mol% $\text{Pd}(\text{PPh}_3)_4$ and 10 equivalents of Na_2CO_3 were refluxed in toluene for 12 h under nitrogen. The reaction mixture was evaporated to dryness and the crude product was purified on a silica-gel column using a solvent mixture of hexane and CH_2Cl_2 as eluent to give an orange target compound.

2g: complex **2f** (100 mg, 0.13 mmol), 4-(diphenylamino)phenylboronic acid (45 mg, 0.16 mmol), 3 mol% $\text{Pd}(\text{PPh}_3)_4$ (5 mg, 0.004 mmol) and Na_2CO_3 (139 mg, 1.31 mol) were used. Yield: 86 mg (71%). $^1\text{H NMR}$ (400 MHz, CDCl_3): $\delta = 8.12$ (s, 1H, C=NH), 8.06 (s, 1H, C=NH), 7.71 (dd, 1H, $J = 7.4, 2.0$ Hz, Ar-H), 7.57 (d, 1H, $J = 2.4$ Hz, Ar-H), 7.39–7.42 (m, 2H, Ar-H), 7.35 (dd, 1H, $J = 7.4, 2.0$ Hz, Ar-H), 7.23–7.25 (m, 4H, Ar-H), 7.09–7.13 (m, 7H, Ar-H), 7.00 (t, 2H, $J = 7.2$ Hz, Ar-H), 3.52–3.58 (m, 2H, cyclohexane-H), 2.62–2.65 (m, 2H, cyclohexane-H), 2.04 (s, 1H, cyclohexane-H), 1.87–1.90 (m, 2H, cyclohexane-H), 1.68 (s, 1H, cyclohexane-H), 1.55 (s, 9H, *tert*-butyl), 1.53 (s, 9H, *tert*-butyl), 1.35–1.36 (m, 2H, cyclohexane-H), 1.30 (s, 9H, *tert*-butyl) ppm. IR (KBr): $\nu = 3435, 2947, 2866, 1607, 1529, 1434, 1319, 1254, 1166, 780$ and 541 cm^{-1} . HRMS (MALDI-TOF, positive mode, CH_2Cl_2): $m/z = 926.4130 [\text{M}]^+$ ($\text{C}_{50}\text{H}_{57}\text{N}_3\text{O}_2\text{Pt}$: calcd $926.4097, \Delta_m = 3.56$ ppm). UV-Vis ($\text{CH}_2\text{Cl}_2, 20^\circ\text{C}$): $\lambda_{\text{max}} [\log(\epsilon \text{ dm}^{-3} \text{ mol}^{-1} \text{ cm}^{-1})] = 259 (4.27), 337 (4.43), 437 (3.48)$ nm. $\text{C}_{50}\text{H}_{57}\text{N}_3\text{O}_2\text{Pt}$ (927.08): calcd C 64.78, H 6.20, N 4.53; found: C 64.56, H 6.17, N 4.32%.

2h: complex **2f** (100 mg, 0.13 mmol), 4-cyanophenylboronic acid (23 mg, 0.16 mmol), 3 mol% $\text{Pd}(\text{PPh}_3)_4$ (5 mg, 0.004 mmol) and Na_2CO_3 (139 mg, 1.31 mol) were used. Yield: 66 mg (64%). $^1\text{H NMR}$ (400 MHz, CDCl_3): $\delta = 8.09$ (s, 1H, C=NH), 8.03 (s, 1H, C=NH), 7.54–7.67 (m, 6H, Ar-H), 7.35 (s, 1H, Ar-H), 7.09 (d, 1H, $J = 2.0$ Hz, Ar-H), 3.54–3.65 (m, 2H, cyclohexane-H), 2.61 (m, 2H, cyclohexane-H), 1.81–1.83 (m, 2H, cyclohexane-H),

1.53–1.55 (m, 18H, *tert*-butyl), 1.27–1.30 (m, 11H, *tert*-butyl and cyclohexane-H), 0.88 (m, 2H, cyclohexane-H) ppm. IR (KBr): $\nu = 3435, 2948, 2867, 2224, 1597, 1531, 1435, 1321, 1255, 1167, 780$ and 543 cm^{-1} . HRMS (MALDI-TOF, positive mode, CH_2Cl_2): $m/z = 785.3370 [\text{M} + \text{H}]^+$ (calcd for $\text{C}_{39}\text{H}_{47}\text{N}_3\text{O}_2\text{Pt} + \text{H}$: $785.3392, \Delta_m = -2.82$ ppm). UV-Vis ($\text{CH}_2\text{Cl}_2, 20^\circ\text{C}$): $\lambda_{\text{max}} [\log(\epsilon \text{ dm}^{-3} \text{ mol}^{-1} \text{ cm}^{-1})] = 248 (4.33), 357 (4.37), 425 (3.59)$ nm. $\text{C}_{39}\text{H}_{47}\text{N}_3\text{O}_2\text{Pt}$ (784.89): calcd C 59.68, H 6.04, N 5.35; found: C 59.65, H 6.12, N 5.28%.

2i: complex **2f** (100 mg, 0.13 mmol), 4-nitrophenylboronic acid (26 mg, 0.16 mmol), 3 mol% $\text{Pd}(\text{PPh}_3)_4$ (5 mg, 0.004 mmol) and Na_2CO_3 (139 mg, 1.31 mol) were used. Yield: 79 mg (75%). $^1\text{H NMR}$ (400 MHz, CDCl_3): $\delta = 8.24$ (d, $J = 8.8$ Hz, 2H, C=NH), 8.19 (s, 1H, C=NH), 8.08 (s, 1H, Ar-H), 7.76 (d, $J = 2.3$ Hz, 1H, Ar-H), 7.65 (d, $J = 8.8$ Hz, 2H, Ar-H), 7.59 (d, $J = 2.3$ Hz, 1H, Ar-H), 7.48 (d, $J = 2.3$ Hz, 1H, Ar-H), 7.12 (d, $J = 2.4$ Hz, 1H, Ar-H), 3.50–3.55 (m, 2H, cyclohexane-H), 2.67–2.73 (m, 2H, cyclohexane-H), 1.93–1.95 (m, 2H, cyclohexane-H), 1.56 (s, 11H, *tert*-butyl and cyclohexane-H), 1.53 (s, 9H, *tert*-butyl), 1.39 (m, 2H, cyclohexane-H), 1.31 (s, 9H, *tert*-butyl) ppm. IR (KBr): $\nu = 3435, 2946, 2867, 1609, 1587, 1509, 1435, 1337, 1255, 1166, 781$ and 544 cm^{-1} . HRMS (MALDI-TOF, positive mode, CH_2Cl_2): $m/z = 804.1544 [\text{M}]^+$ ($\text{C}_{38}\text{H}_{47}\text{N}_3\text{O}_4\text{Pt}$: calcd $804.8755, \Delta_m = 8.97$ ppm). UV-Vis ($\text{CH}_2\text{Cl}_2, 20^\circ\text{C}$): $\lambda_{\text{max}} [\log(\epsilon \text{ dm}^{-3} \text{ mol}^{-1} \text{ cm}^{-1})] = 266 (3.61), 357 (4.30), 431 (4.32)$ nm. $\text{C}_{38}\text{H}_{47}\text{N}_3\text{O}_4\text{Pt}$ (804.88): calcd C 56.71, H 5.89, N 5.22; found: C 56.47, H 5.69, N 5.13%.

2j: complex **2f** (100 mg, 0.13 mmol), 9,9-dihexyl-9H-fluoren-2-ylboronic acid (59 mg, 0.16 mmol), 3 mol% $\text{Pd}(\text{PPh}_3)_4$ (5 mg, 0.004 mmol) and Na_2CO_3 (139 mg, 1.31 mol) were used. Yield: 57 mg (43%). $^1\text{H NMR}$ (400 MHz, CDCl_3): $\delta = 8.17$ (s, 1H, C=NH), 8.06 (s, 1H, C=NH), 7.82 (s, 1H, Ar-H), 7.64–7.65 (m, 2H, Ar-H), 7.58 (s, 1H, Ar-H), 7.45–7.48 (m, 3H, Ar-H), 7.28–7.33 (m, 3H, Ar-H), 7.09 (s, 1H, Ar-H), 3.57–3.60 (m, 2H, cyclohexane-H), 2.56 (m, 2H, cyclohexane-H), 1.89–1.98 (m, 8H), 1.54–1.59 (m, 18H, *tert*-butyl), 1.25–1.39 (m, 15H), 1.05 (m, 12H), 0.76 (s, 6H, $-\text{CH}_3$) ppm. IR (KBr): $\nu = 3435, 2952, 2856, 1605, 1527, 1434, 1318, 1254, 1167, 780$ and 582 cm^{-1} . HRMS (MALDI-TOF, positive mode, CH_2Cl_2): $m/z = 1015.5505 [\text{M}]^+$ ($\text{C}_{57}\text{H}_{76}\text{N}_2\text{O}_2\text{Pt}$: calcd $1015.5553, \Delta_m = -4.73$ ppm). UV-Vis ($\text{CH}_2\text{Cl}_2, 20^\circ\text{C}$): $\lambda_{\text{max}} [\log(\epsilon \text{ dm}^{-3} \text{ mol}^{-1} \text{ cm}^{-1})] = 287 (4.28), 342 (4.50), 432 (3.67)$ nm. $\text{C}_{57}\text{H}_{76}\text{N}_2\text{O}_2\text{Pt}$ (1016.3): calcd C 67.36, H 7.54, N 2.76; found: C 67.41, H 7.52, N 2.79%.

Acknowledgements

We thank Hong Kong Baptist University (FRG2/11-12/0071) and Hong Kong Research Grants Council (HKBU 202308) for the financial support. W.-K.W. and W.-Y.W. also thank a grant from Areas of Excellence Scheme, University Grants Committee, Hong Kong (Project No. [AoE/P-03/08]). W.-Y.W. also acknowledges the financial support from Hong Kong Research Grants Council (HKUST2/CRF/10).

Notes and references

- C. W. Tang and S. A. S. Van Slyke, *Appl. Phys. Lett.*, 1987, **51**, 913.
- J. H. Burroughes, D. D. C. Bradley, A. R. Brown, R. N. Marks, K. Mackay, P. L. Burns and A. B. Holmes, *Nature*, 1990, **347**, 539.
- (a) M. A. Baldo, M. E. Thompson and S. R. Forrest, *Nature*, 2000, **403**, 750; (b) C. Adachi, M. A. Baldo, S. R. Forrest and

- M. E. Thompson, *Appl. Phys. Lett.*, 2000, **77**, 904; (c) M. A. Baldo, S. Lamansky, P. E. Burrows, M. E. Thompson and S. R. Forrest, *Appl. Phys. Lett.*, 1999, **75**, 4; (d) M. A. Baldo, D. F. O'Brien, Y. You, A. Shoustikov, S. Sibley, M. E. Thompson and S. R. Forrest, *Nature*, 1998, **395**, 151.
- 4 (a) Y. C. Zhu, L. Zhou, H. Y. Li, Q. L. Xu, M. Y. Teng, Y. X. Zheng, J. L. Zuo, H. J. Zhang and X. Z. You, *Adv. Mater.*, 2011, **23**, 4041; (b) Q. Zhao, C. H. Huang and F. Y. Li, *Chem. Soc. Rev.*, 2011, **40**, 2508; (c) Y. J. Pu, N. Iguchi, N. Aizawa, H. Sasabe, K. Nakayama and J. Kido, *Org. Electron.*, 2011, **12**, 2103; (d) C. H. Hsieh, F. I. Wu, C. H. Fan, M. J. Huang, K. Y. Lu, P. Y. Chou, Y. H. O. Yang, S. H. Wu, I. C. Chen, S. H. Chou, K. T. Wong and C. H. Cheng, *Chem.–Eur. J.*, 2011, **17**, 9180; (e) Y. N. Hong, J. W. Y. Lam and B. Z. Tang, *Chem. Soc. Rev.*, 2011, **40**, 5361; (f) S. Fantacci and F. De Angelis, *Coord. Chem. Rev.*, 2011, **255**, 2704; (g) P. T. Chou, Y. Chi, M. W. Chung and C. C. Lin, *Coord. Chem. Rev.*, 2011, **255**, 2653; (h) S. M. Chen, G. P. Tan, W. Y. Wong and H. S. Kwok, *Adv. Funct. Mater.*, 2011, **21**, 3785; (i) Z. Q. Chen, Z. Q. Bian and C. H. Huang, *Adv. Mater.*, 2010, **22**, 1534; (j) G. J. Zhou, Q. Wang, W. Y. Wong, D. G. Ma, L. X. Wang and Z. Y. Lin, *J. Mater. Chem.*, 2009, **19**, 4457; (l) T. Tsuzuki and S. Tokito, *Appl. Phys. Lett.*, 2009, **94**, 033302; (m) C. X. Li, G. H. Zhang, H. H. Shih, X. Q. Jiang, P. P. Sun, Y. Pan and C. H. Cheng, *J. Organomet. Chem.*, 2009, **694**, 2415–2420; (n) J. J. Kim, Y. You, Y. S. Park, J. J. Kim and S. Y. Park, *J. Mater. Chem.*, 2009, **19**, 8347; (o) S. C. Lo, R. N. Bera, R. E. Harding, P. L. Burn and I. D. W. Samuel, *Adv. Funct. Mater.*, 2008, **18**, 3080; (p) D. M. Kang, J. W. Kang, J. W. Park, S. O. Jung, S. H. Lee, H. D. Park, Y. H. Kim, S. C. Shin, J. J. Kim and S. K. Kwon, *Adv. Mater.*, 2008, **20**, 2003.
- 5 (a) B. P. Yan, C. C. C. Cheung, S. C. F. Kui, H. F. Xiang, V. A. L. Roy, S. J. Xu and C. M. Che, *Adv. Mater.*, 2007, **19**, 3599; (b) X. H. Yang, Z. X. Wang, S. Madakuni, J. Li and G. E. Jabbour, *Adv. Mater.*, 2008, **20**, 2405; (c) Z. B. Wang, M. G. Helander, Z. M. Hudson, J. Qiu, S. Wang and Z. H. Lu, *Appl. Phys. Lett.*, 2011, **98**, 073310; (d) K. Li, X. G. Guan, C. W. Ma, W. Lu, Y. Chen and C. M. Che, *Chem. Commun.*, 2011, **47**, 9075; (e) Y. Chi and P. T. Chou, *Chem. Soc. Rev.*, 2010, **39**, 638; (f) A. G. Williams, *Chem. Soc. Rev.*, 2009, **38**, 1783; (g) W. Y. Wong and C. L. Ho, *Coord. Chem. Rev.*, 2009, **253**, 1709; (h) P. T. Furuta, L. Deng, S. Garon, M. E. Thompson and J. M. J. Frechet, *J. Am. Chem. Soc.*, 2004, **126**, 15388; (i) N. Komiya, M. Okada, K. Fukumoto, D. Jomori and T. Naota, *J. Am. Chem. Soc.*, 2011, **133**, 6493; (j) W. Lu, B. X. Mi, M. C. W. Chan, Z. Hui, C. M. Che, N. Y. Zhu and S. T. Lee, *J. Am. Chem. Soc.*, 2004, **126**, 4958.
- 6 (a) Y. L. Tung, S. W. Lee, Y. Chi, L. S. Chen, C. F. Shu, F. I. Wu, A. J. Carty, P. T. Chou, S. M. Peng and G. M. Lee, *Adv. Mater.*, 2005, **17**, 1059; (b) C. H. Lin, C. W. Hsu, J. L. Liao, Y. M. Cheng, Y. Chi, T. Y. Lin, M. W. Chung, P. T. Chou, G. H. Lee, C. H. Chang, C. Y. Shih and C. L. Ho, *J. Mater. Chem.*, 2012, **22**, 10684; (c) B. S. Du, J. L. Liao, M. H. Huang, C. H. Lin, H. W. Lin, Y. Chi, H. A. Pan, G. L. Fan, K. T. Wong, G. H. Lee and P. T. Chou, *Adv. Funct. Mater.*, 2012, DOI: 10.1002/adfm.201200718.
- 7 K. Li, X. G. Guan, C. W. Ma, W. Lu, Y. Chen and C. M. Che, *Chem. Commun.*, 2011, **47**, 9075.
- 8 (a) C. M. Che, S. C. Chan, H. F. Xiang, M. C. W. Chan, Y. Liu and Y. Wang, *Chem. Commun.*, 2004, 1484; (b) C. M. Che, C. C. Kwok, S. W. Lai, A. F. Rausch, W. J. Finkenzerler, N. Y. Zhu and H. Yersin, *Chem.–Eur. J.*, 2010, **16**, 233.
- 9 (a) W. K. Lo, W. K. Wong, J. P. Guo, W. Y. Wong, K. F. Li and K. W. Cheah, *Inorg. Chim. Acta*, 2004, **357**, 4510; (b) W. K. Lo, W. K. Wong, W. Y. Wong, J. P. Guo, K. T. Yeung, Y. K. Cheng, X. P. Yang and R. A. Jones, *Inorg. Chem.*, 2006, **45**, 9315; (c) X. P. Yang, R. A. Jones, Q. Y. Wu, M. M. Oye, W. K. Lo, W. K. Wong and A. L. Holmes, *Polyhedron*, 2006, **25**, 271; (d) W. Y. Bi, X. Q. Lu, W. L. Chai, J. R. Song, W. K. Wong, X. P. Yang and R. A. Jones, *Z. Anorg. Allg. Chem.*, 2008, **634**, 1795.
- 10 (a) H. F. Xiang, S. C. Chan, K. K. Y. Wu, C. M. Che and P. T. Lai, *Chem. Commun.*, 2005, 1408; (b) F. Galbrecht, X. H. Yang, B. S. Nehls, D. Neher, T. Farrell and U. Scherf, *Chem. Commun.*, 2005, 2378.
- 11 (a) M. Holbach, X. L. Zheng, C. Burd, C. W. Jones and M. Weck, *J. Org. Chem.*, 2006, **71**, 2903; (b) E. J. Campbell and S. T. Nguyen, *Tetrahedron Lett.*, 2001, **42**, 1221.
- 12 (a) X. C. Wang, H. Q. Wang, Y. Yang, Y. J. He, L. Zhang, Y. F. Li and X. Y. Li, *Macromolecules*, 2010, **43**, 709; (b) M. Y. Yuen, S. C. E. Kui, K. H. Low, C. C. Kwok, S. S. Y. Chui, C. W. Ma, N. Y. Zhu and C. M. Che, *Chem.–Eur. J.*, 2010, **16**, 14131.
- 13 B. W. D'Andrade, R. J. Holmes and S. R. Forrest, *Adv. Mater.*, 2004, **16**, 624.
- 14 (a) A. Y. Y. Tam, D. P. K. Tsang, M. Y. Chan, N. Y. Zhu and V. W. W. Yam, *Chem. Commun.*, 2011, **47**, 3383; (b) G. J. Zhou, Q. Wang, X. Z. Wang, C. L. Ho, W. Y. Wong, D. G. Ma, L. X. Wang and Z. Y. Lin, *J. Mater. Chem.*, 2010, **20**, 7472.
- 15 (a) H. B. Wu, G. J. Zhou, J. H. Zou, C. L. Ho, W. Y. Wong, W. Yang, J. B. Peng and Y. Cao, *Adv. Mater.*, 2009, **21**, 4181; (b) G. J. Zhou, Q. Wang, C. L. Ho, W. Y. Wong, D. G. Ma and L. X. Wang, *Chem. Commun.*, 2009, 3574; (c) G. J. Zhou, W. Y. Wong and X. L. Yang, *Chem.–Asian J.*, 2011, **6**, 1706; (d) G. J. Zhou, W. Y. Wong and S. Suo, *J. Photochem. Photobiol., C*, 2010, **11**, 133; (e) B. Zhang, G. Tan, C.-S. Lam, B. Yao, C.-L. Ho, Z. Xie, W.-Y. Wong, J. Ding and L. Wang, *Adv. Mater.*, 2012, **24**, 1873.
- 16 L. F. Groux, T. Weiss, D. N. Reddy, P. A. Chase, W. E. Piers, T. Ziegler, M. Parvez and J. Benet-Buchholz, *J. Am. Chem. Soc.*, 2005, **127**, 1854.
- 17 F. R. Heirtzler, M. J. Howard and S. I. G. Dias, *J. Org. Chem.*, 2008, **73**, 2548.
- 18 Z. W. Liu, Z. Q. Bian, F. Hao, D. B. Nie, F. Ding and C. Hs Huang, *Org. Electron.*, 2009, **10**, 247.